Optimization II - Optimal vaccination

Olav Milian Schmitt Gran, Tor Ola Ousdal Solheim,
Ulrik Røssevold Flem

April 2021

Abstract

With COVID-19 still raging across the world, vaccines are currently in the spotlight. In this paper, we want to find the optimal vaccination strategy in the SIR model. First, we introduce and prove results about the SIR model. Next, we introduce two different cost functionals to find an optimal vaccination strategy. We find the optimality system and numerically solve for the vaccination strategy using a projected gradient method. The experiment was successful for both cost-functionals and the results are similar to those of earlier works.

1 Introduction

In the days of a worldwide pandemic and full-scale mass vaccination efforts, it is important to administer vaccines as efficiently as possible so as to minimize fatalities and costs incurred by society as a result of an ongoing pandemic. This is what we aim to provide with this paper. While the primary restricting factor for the mass-production and distribution of COVID-19 vaccines has been production and distribution time as opposed to production and distribution costs, it is nevertheless interesting to investigate an optimal vaccination protocol where costs of production and distribution are factored in. This is at its core a toy example, as simulating the spread of real-world infectious diseases are more complicated than what will be assumed here. However, we believe that any information is better than none. In addition, while this may not accurately describe the ongoing COVID-19 pandemic, it may still be useful for describing the spread of a disease in less complicated scenarios, such as in the case of a locally confined disease, e.g. a disease spreading through a village or school.

The model we will use is known as the SIR model. This is a coupled system of three nonlinear ordinary differential equations, wherein the population is split into susceptible (S), infected (I) and recovered (R) individuals. The SIR model then tracks how these states evolve over time given some initial conditions and system parameters. This is the basis for the models developed by government health organizations around the world. Again we'd like to emphasize that this is at its core a toy example, as the models used by governments and NGO's alike are typically much more sophisticated, taking into account things like different population groups, mutations and the specific interactions between members of the population (e.g. compartment-models, which attempts to take close-contacts into account by splitting the population into compartments, where there is a lot of interaction within each compartment, but less interaction between compartment). For more information on such models, see [1].

In this work we will first explore the SIR model with vaccination, explain it, simulate it and prove existence and uniqueness of solutions. Then, we will introduce a cost functional and turn this problem into an optimization problem. Lastly we will numerically solve this optimization problem and provide an optimal vaccination strategy.

2 SIR model

2.1 The SIR model

The SIR model is a nonlinear system of three ODEs solving for the susceptible population, S(t), the infected population, I(t), and the recovered population,

R(t). It has the form

$$\begin{aligned} \frac{dS}{dt} &= N\nu - (\nu + u(t))S(t) - \frac{\beta}{N}S(t)I(t) \text{ , } S(0) = S_0 \geq 0 \\ \frac{dI}{dt} &= \frac{\beta}{N}S(t)I(t) - (\gamma + \nu)I(t) \text{ , } I(0) = I_0 \geq 0 \\ \frac{dR}{dt} &= \gamma I(t) - \nu R(t) + u(t)S(t) \text{ , } R(0) = R_0 \geq 0 \end{aligned} \tag{1}$$

where N is the total population, ν is the birth and death rate, $u(t)$ is fraction of susceptible population vaccinated per time, β is the rate of transmission, and γ is the rate of recovery.

Notice that since the birth and death rate is assumed to be the same, the total population doesn't change and $S(t) + I(t) + R(t) = N$ for all t. The people making up the population, however, will change over time.

In this model, it is assumed that those who recover or are vaccinated can never be infected again. Furthermore, spreading of the disease is assumed to be proportional to both $I(t)$ and $S(t)$, with proportionality constant $\frac{\beta}{N}$. This constant can be understood as the rate at which the fraction of infected population infects the susceptible population.

For this problem to be well-defined, we need $u(t)$ to belong to the admissible set given by

$$U_{ad} = \{u(t) : \text{u is measurable and } 0 \leq u(t) \leq 0.9 \text{ for all t}\}. \tag{2}$$

The paper [5] claims that vaccinating more than 90% of the susceptible population at any given time-step is impossible in real-world scenarios. This is not really true, as one could imagine a scenario (say, near the end of a dying epidemic) where very few people remain susceptible. In an extreme case, we could consider the situation of having only a single susceptible person in the population. In such a case, vaccinating 100% of the susceptible population must be possible if it is possible to vaccinate anyone at all, since vaccinating 100% of the susceptible population in this case amounts to vaccinating a single person. That being said, we choose to keep this upper bound of 90% in our treatment for cross-consistency with the aforementioned paper. Furthermore, the functions S, I, R are assumed to come from the Hilbert space $H^1(0, T)$. They certainly need to be differentiable, and as will be shown in 2.3, uniqueness requires their square to also lie in $L^1(0, T)$, where T is the endtime of the model. Hence the functions themselves need only lie in $L^2(0, T)$.

2.2 Existence of solution

We wish to show that given some vaccination protocol $u(t) \in U_{ad}$, the system admits a unique solution. First we want to look at the existence of a solution. The system can be described as

$$\mathbf{y}_t = \mathbf{f}(t, S, I, R) \text{ , } \mathbf{y}(0) = \mathbf{y}_0,$$

where $\mathbf{y}(t)$ is a vector in $\mathbb{R}^3$ with components S, I and R. Let $\mathbf{f}$ be defined on the rectangular domain

$$D = \{(t, S, I, R) : |t| \leq T, |S| \leq N, |I| \leq N, |R| \leq N\}$$

Will prove existence using Caratheodory's theorem of existence. It states that given such a system, if $\mathbf{f}$ is Caratheodory as well as majorant, then the system admits an absolutely continuous solution almost everywhere in D.

Firstly, the function $t \to \mathbf{f}(t, S, I, R)$ is clearly measurable as $u(t)$, as well as $S(t)$, $I(t)$ and $R(t)$ are assumed to be measurable. Secondly, the functions $d\mathbf{f}/dS$, $d\mathbf{f}/dI$ and $d\mathbf{f}/dR$ all exists for every (S, I, R) in D, hence $\mathbf{f}$ is continuous in D wrt. S, I and R. By these two statements, $\mathbf{f}(t, S, I, R)$ is a Caratheodory function.

Next we want to prove that $\mathbf{f}$ is majorant. This means finding a Lebesgue-integrable function $m(t)$ from D to $\mathbb{R}^3$ which satisfies $|\mathbf{f}(t, S, I, R)| \leq m(t)$ in D.

By using the relation that $S + I + R = N$ for all t, we can bound each component of $\mathbf{f}$ using the original relation $S \leq N$, $I \leq N$ and $R \leq N$. This gives:

$$\left|\frac{dS(t)}{dt}\right| \leq (2\nu + \beta + 0.9)N$$

$$\left|\frac{dI(t)}{dt}\right| \leq (\beta + \gamma + \nu)N$$

$$\left|\frac{dR(t)}{dt}\right| \leq (\gamma + \nu + 0.9)N$$

From this it follows that

$$|\mathbf{f}(t, S, I, R)| = \sqrt{\left|\frac{dS(t)}{dt}\right|^2 + \left|\frac{dI(t)}{dt}\right|^2 + \left|\frac{dR(t)}{dt}\right|^2}$$

$$\leq \sqrt{(2\nu + \beta + 0.9)^2 N^2 + (\beta + \gamma + \nu)^2 N^2 + (\gamma + \nu + 0.9)^2 N^2}$$

$$= C \cdot N,$$

where $C = \sqrt{(2\nu + \beta + 0.9)^2 + (\beta + \gamma + \nu)^2 + (\gamma + \nu + 0.9)^2} < \infty$.

Thus, let $m(t) = C \cdot N$, giving $m(t) \geq |\mathbf{f}(t, S, I, R)|$ in D, and we get that $\mathbf{f}$ is majorant. By the Caratheodory existence theorem we then get the existence of an absolutely continuous solution of the problem almost everywhere in D.

2.3 Uniqueness of solutions

Uniqueness of the solution can be proven using the Gronwall inequality which states that if a function can be expressed as

$$y^2(t) \leq C_1 \int_0^t y^2(\xi) d\xi + C_2,$$

for some positive constants C_1 and C_2, then one gets that

$$y^2(t) \leq C_2 \left(1 + C_1 t e^{C_2 t}\right).$$

In the case that $C_2 = 0$, then $y^2(t) = 0$ for a.e. t.

Define now two different admissable vaccination functions u_1 and u_2. By existence, there will then exist solutions y_1 and y_2 as well. Define then the new functions $u = u_1 - u_2$, $S = S_1 - S_2$, $I = I_1 - I_2$ and $R = R_1 - R_2$. Inserting these into the SIR model gives the new equations:

$$\begin{aligned} S_t &= -\nu S - \frac{\beta}{N}(I_1 S_1 - I_2 S_2) - u_1 S_1 + u_2 S_2 \ , \ S(0) = 0 \\ I_t &= \frac{\beta}{N}(I_1 S_1 - I_2 S_2) - (\gamma + \nu) I \ , \ I(0) = 0 \\ R_t &= \gamma I - \nu R + u_1 S_1 - u_2 S_2 \ , \ R(0) = 0 \end{aligned}$$

Looking at the equation for S_t first. Since $S \geq 0$ and $\nu \geq 0$ we get:

$$\begin{aligned} S_t &\leq \frac{\beta}{N}(I_1 S_1 - I_2 S_2) - u_1 S_1 + u_2 S_2 \\ &= \frac{\beta}{N}(I_1 S_1 - I_1 S_2 + I_1 S_2 - I_2 S_2) - u_1 S_1 + u_1 S_2 - u_1 S_2 + u_2 S_2 \\ &= \underline{\frac{\beta}{N}(I_1 S + S_2 I) - u_1 S - u S_2} \end{aligned}$$

Now multiply with S and integrate from 0 to t, getting the equation in weak form with S as test function. We can do this, as in weak form, the test function can be any function in $H^1(0,T)$. This gives:

$$\int_0^t S_\xi S d\xi \leq \frac{\beta}{N} \int_0^t I_1 S^2 d\xi + \frac{\beta}{N} \int_0^t S_2 I S d\xi - \int_0^t u_1 S^2 - \int_0^t S_2 u S d\xi$$

To write this in an understandable way, will need Young's and Hölder's inequalities. Young's inequality states that for real numbers a and b we have $ab \leq \frac{a^2}{2} + \frac{b^2}{2}$. Hölder's inequality states that for measurable functions f and g we have $||fg||_{L^1(0,t)} \leq ||f||_{L^p(0,t)} ||g||_{L^q(0,t)}$, where p and q are conjugated exponentials.

For the lefthand side, notice that $S_\xi S = \frac{1}{2} \frac{d}{d\xi} S^2$. Inserting this and solving the integral we then get $\int_0^t S_\xi S d\xi = \frac{1}{2} \left[S^2(t) - S^2(0)\right] = \frac{1}{2} S^2(t)$ as $S(0) = 0$.

For the following, note that the integrals on the lefthand side all have positive integrands, meaning e.g. $I_1S^2 = |I_1S^2|$. Furthermore all $S_i(t)$, $I_i(t)$ and $R_i(t)$ are uniformly bounded by N while $u_i(t)$ is uniformly bounded by 0.9. In particular, $u(t)$ is bounded by 1, so will use that bound to get nicer results.

Applying Hölder's inequality to the first l.h.s (lefthand side) integral, we get

$$\begin{aligned}\frac{\beta}{N}\int_0^t I_1S^2d\xi &\leq \frac{\beta}{N}||I_1||_{L^\infty(0,t)}||S^2||_{L^1(0,t)}\\ &\leq \underline{\beta||S^2||_{L^1(0,t)}}\end{aligned}$$

For the second l.h.s. integral, need to first use Young's inequality on IS. Then get $IS \leq \frac{1}{2}I^2 + \frac{1}{2}S^2$. This leads to

$$\frac{\beta}{N}\int_0^t S_2ISd\xi \leq \frac{\beta}{2N}\int_0^t S_2I^2d\xi + \frac{\beta}{2N}\int_0^t S_2S^2d\xi.$$

Applying Hölder's inequality to these two integrals we get

$$\frac{\beta}{N}\int_0^t S_2ISd\xi \leq \frac{\beta}{2}||I^2||_{L^1(0,t)} + \frac{\beta}{2}||S^2||_{L^1(0,t)}.$$

Continue this procedure for the two final l.h.s. integrals, finally giving the total inequality:

$$\frac{1}{2}S^2(t) \leq \left(\frac{3\beta}{2} + \frac{N+2}{2}\right)||S^2||_{L^1(0,t)} + \frac{\beta}{2}||I^2||_{L^1(0,t)} + \frac{N}{2}||u^2||_{L^1(0,t)}.$$

The treatment of the equations for $I(t)$ and $R(t)$ are identical, and we will therefore only present the final inequalities. They turn out to be

$$\frac{1}{2}I^2(t) \leq \frac{\beta}{2}||S^2||_{L^1(0,t)} + \frac{3\beta}{2}||I^2||_{L^1(0,t)}$$

for $I(t)$, and

$$\frac{1}{2}R^2(t) \leq \frac{1}{2}||S^2||_{L^1(0,t)} + \frac{\gamma}{2}||I^2||_{L^1(0,t)} + \left(\frac{\gamma}{2} + \nu + \frac{N+2}{2}\right)||R^2||_{L^1(0,t)} + \frac{N}{2}||u^2||_{L^1(0,t)}$$

for $R(t)$. Next we will use the fact that $S^2 + I^2 + R^2 = y^2$. Therefore, by adding up all three inequalities, we get

$$\begin{aligned}&y^2(t) \leq (4\beta + N + 3)||S^2||_{L^1(0,t)} + (4\beta+\gamma)||I^2||_{L^1(0,t)} + (\gamma + 2\nu + N + 1)||R^2||_{L^1(0,t)} + 2N||u^2||_{L^1(0,t)}\\ &\leq (8\beta + 2\gamma + 2\nu + 2N + 4)\left(||S^2||_{L^1(0,t)} + ||I^2||_{L^1(0,t)} + ||R^2||_{L^1(0,t)}\right) + 2N||u^2||_{L^1(0,t)}\\ &= \underline{C_1\int_0^t y^2(\xi)d\xi + C_2},\end{aligned}$$

where we defined $C_1 = (8\beta + 2\gamma + 2\nu + 2N + 4)$ and $C_2 = 2N||u^2||_{L^1(0,t)}$. Furthermore, the expression for C_1 was achieved by using $ax + by + cz \leq (a + b + c)(x + y + z)$ when all parameters are positive. Moreover, since $S, I, R \geq 0$, we have $||S^2||_{L^1(0,t)} + ||I^2||_{L^1(0,t)} + ||R^2||_{L^1(0,t)} = ||y^2||_{L^1(0,t)}$.

This equation is now in the form to use Gronwall's inequality. Then get:

$$y^2(t) \leq 2N||u^2||_{L^1(0,t)} \left(1 + C_1 t e^{2N||u^2||_{L^1(0,t)} \cdot t}\right).$$

Now, as $u_1 \to u_2$, $u \to 0$, which means $C_2 \to 0$. Hence $y^2(t) = 0$ almost everywhere. Thus,

$$y^2(t) = [y_1(t) - y_2(t)]^2 = 0 \implies \underline{\underline{y_1(t) = y_2(t)}},$$

which proves the solution must be unique for a given vaccination $u(t)$ Hence, the SIR model admits a unique, absolutely continuous solution for almost every time, t.

2.4 Numerical solution of SIR-vaccination model

We solve the state equation (1) using a 4th-order explicit Runge-Kutta method. This iterative scheme updates the solution y at the next timestep according to

$$y_{n+1} = y_n + \frac{h}{6}\left(k_1 + 2k_2 + 2k_3 + k_4\right), \tag{3}$$

where $\{k_1, k_2, k_3, k_4\}$ are given by

$$\begin{aligned} k_1 &= f(t_n, y_n) \\ k_2 &= f\left(t_n + \frac{h}{2}, y_n + h\frac{k_1}{2}\right) \\ k_3 &= f\left(t_n + \frac{h}{2}, y_n + h\frac{k_2}{2}\right) \\ k_4 &= f(t_n + h, y_n + hk_3) \end{aligned} \tag{4}$$

In our particular case, the solution $\mathbf{y}_n$ at timestep t_n is a vector containing the numerical solutions to the three states $S(t_n), I(t_n), R(t_n)$ at said timestep t_n. That is, we have $\mathbf{y}_n = \begin{bmatrix} S_n & I_n & R_n \end{bmatrix}^\top$. Similarly, the right-hand-side $\mathbf{f}(t_n, \mathbf{y_n})$ is a vector of functions, given by

$$\mathbf{f}(t_n, \mathbf{y}_n) = \begin{bmatrix} f_1(t_n, \mathbf{y}_n) \\ f_2(t_n, \mathbf{y}_n) \\ f_3(t_n, \mathbf{y}_n) \end{bmatrix} = \begin{bmatrix} N\nu - (\nu + u_n)S_n - \frac{\beta}{N} S_n I_n \\ \frac{\beta}{N} S_n I_n - \nu I_n - \gamma I_n \\ \gamma I_n - \nu R_n + u_n S_n \end{bmatrix} \tag{5}$$

This is a fourth order method, meaning that the local truncation error is of order $\mathcal{O}(h^5)$ and the global truncation error is of order $\mathcal{O}(h^4)$. Note that we also use a backwards-in-time RK4 solver to solve the adjoint equation.

Investigating the stability of this explicit RK4 method, while surely important, has not been a major focus in this project. For those particularly interested in the stability of an explicit RK4 method, we refer the reader to the book by Alfio Quarteroni, Riccardo Sacco and Fausto Saleri *Numerical Mathematics, Second Edition*, [2], where on page 527 there is a plot showing A-stability of explicit Runge-Kutta methods of order 1 up to and including order 4.

2.5 Vaccination protocols

Before we investigate the optimal control problem, we want to investigate the effect of different vaccination protocols heuristically through a few motivating examples. As previously noted, $u(t)$ is the proportion of the susceptible population $S(t)$ being vaccinated at the given timestep t. By considering different function expressions for the term $u(t)$, we may simulate various vaccination protocols. Given the potential real-world applications of the SIR model, we find it most pertinent to investigate vaccination protocols which could feasibly be implemented in the real-world.

In the spirit of feasibility, consider the following basic vaccination protocol: Every day, a constant number of people are being vaccinated. Recall that the number of susceptibles $S(t)$ changes from one timestep to the next as more and more people enter the recovered state, either by way of infection or vaccination. With a constant supply of vaccines, this would imply that as the number of susceptibles decrease, we may vaccinate a larger proportion of the susceptibles, and vice versa. In other words, with a constant supply of vaccines, the vaccination rate $u(t)$ and the number of susceptibles $S(t)$ are inversely proportional, yielding the relationship

$$u(t)S(t) = k, \tag{6}$$

where k is some fixed constant corresponding to the number of people we can vaccinate at every timestep. We wish to test this vaccination strategy for a scenario reminiscent of Norway's dealings with the pandemic. In particular, we will assume an initial susceptible population $S_0 = 5,328,000$, an initial recovered/immune population of zero, and a single infected individual. Moreover, we assume that an infected individual recovers after roughly 14 days, the reciprocal of which yields our recovery rate $\gamma = 0.07$. In addition, we assume an equal birth- and death rate $v = 128/N$, N being the total population. According to SSB [3], [4], there are an average of 145 births and 111 deaths every day in Norway. Since we want the birth- and death rate in our model to be equal, we set it equal to the average of Norway's birth- and death rates, yielding an average of 128 births and 128 deaths per day. Lastly, we assume a a basic reproduction number of $K = 2.87$ for the disease. The disease reproduction rate β is then recovered as $\beta = K(\gamma + v)$, yielding $\beta = 0.201$. The results are given

in the following plots, where we also include for reference a plot showing the case of no vaccination protocol.

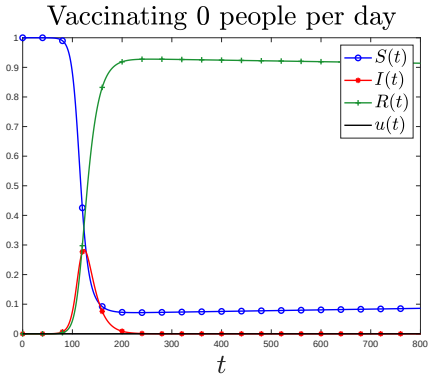

(a) No vaccination protocol

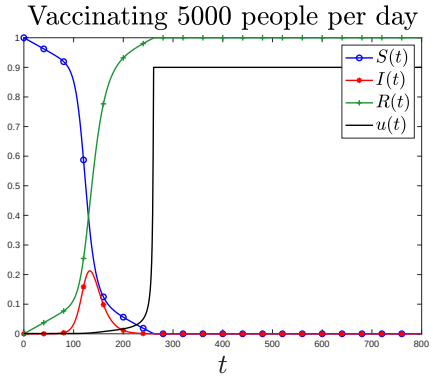

(b) 5,000 vaccinated per day

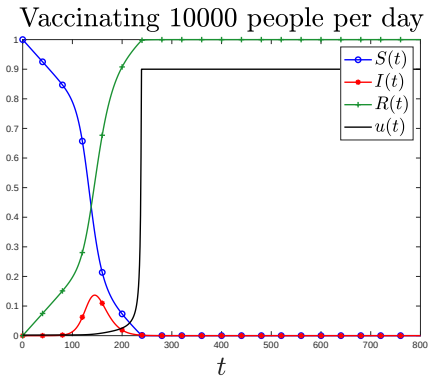

(c) 10,000 vaccinated per day

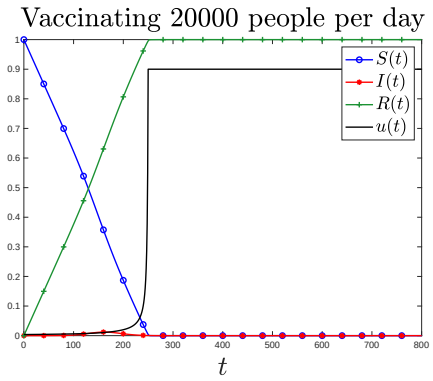

(d) 20,000 vaccinated per day

Figure 1: Constant Vaccination protocols

Observe that as we vaccinate more and more people every day from the moment of the first recorded infection, we are able to significantly flatten the curve. Observe that when vaccinating 20,000 people per day from the start of the outbreak, the disease hardly spreads.

Though the vaccination protocol hitherto described is realistic in a general sense, it is not realistic for the case of a newly discovered disease (as is the case with the ongoing COVID-19 pandemic), since the aforementioned vaccination protocol presupposes availability of the vaccine at the start of the outbreak. This is typically the case for e.g. flu vaccines, where vaccines are prepared prior to the flu season. For the case of a newly discovered disease for which there exists no vaccine at the time of outbreak (as is the case for COVID-19),

it is more realistic with a ramping vaccination protocol. That is, at the start of the outbreak, we have no vaccine, and can therefore not vaccinate anyone. As time marches on, research, development and testing of the vaccine is carried out, and eventually a vaccine is available. Once available, production- and distribution capacities start out low, and correspondingly few people are vaccinated. However, as time moves on further still, more and more people are vaccinated each day as production and distribution capacities increase until some maximum is reached. We can represent this scenario through the following relation between $u(t)$ and $S(t)$

$$u(t)S(t) = k(t), \tag{7}$$

where $k(t)$ is the total number of people we have the capacity to vaccinate on any given day. Observe that now, $k(t)$ is no longer constant, but rather a function of time. In particular, we specify some starting time for the vaccination protocol, and some time at which the vaccinations are carried out at full capacity. $k(t)$ is then simply the straight-line function of t with slope and intercept such that the aforementioned specifications are respected. We tested this vaccination protocol on the same system as before, using the maximum-capacity values of $k_{\max} = 5,000$, $k_{\max} = 10,000$ and $k_{\max} = 20,000$. Again we include for reference the case when no vaccination protocol is implemented.

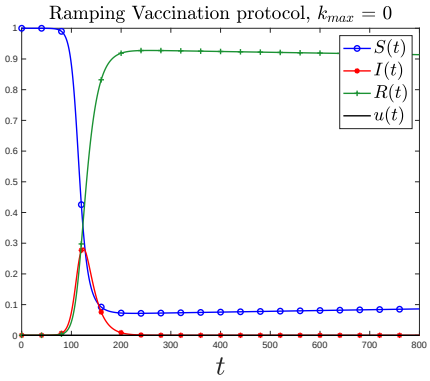

(a) No vaccination protocol

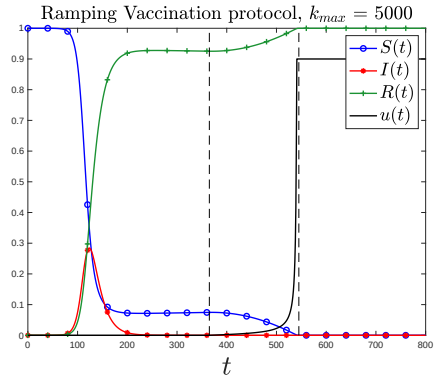

(b) Maximum capacity: 5,000 vaccinations per day

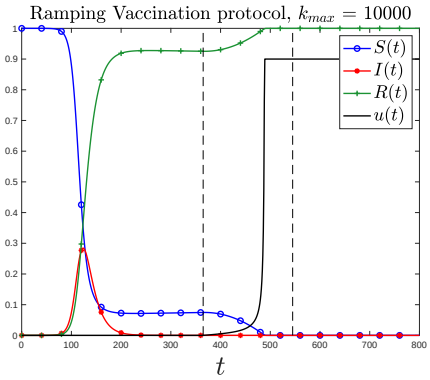

(c) Maximum capacity: 10,000 vaccinations per day

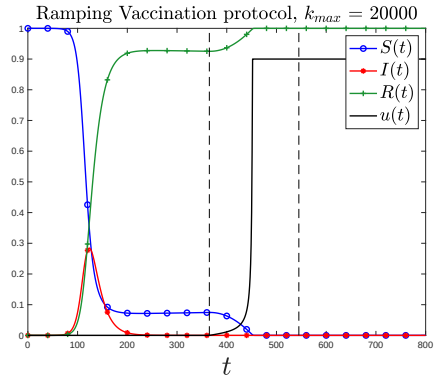

(d) Maximum capacity: 20,000 vaccinations per day

Figure 2: Ramping Vaccination protocols. Vaccination starts 1 year after the outbreak, and reaches full capacity 6 months later. These 6 months are indicated by the vertical dashed lines.

Since the SIR model explored herein yields only a single epidemic "wave" (due in part to the assumption that recovered people are immune for life), we see that the ramping vaccination protocol has little to offer: By the time the vaccine is available, the pandemic has already died down. We do notice, however, that the number of susceptibles tends towards zero as new people born into the susceptible state are continuously being vaccinated. In the case of no vaccination, these newborn people would simply remain in the susceptible state indefinitely in lieu of another outbreak. Thus we arrive at the painfully trivial conclusion that it would be better to have a vaccine ready before the outbreak hits, as opposed to after the fact. One should take this result with a fistful of salt; as we're all well aware, there may be multiple waves in a given

pandemic. Thus, if any subsequent waves hit during the ramping-stage (or even better, once we've reached full capacity) the effect of a ramping vaccine protocol will be more in line with those in Figure 1. Having explored the effect of two reasonable vaccination strategies, we proceed with investigating the optimal control problem.

3 Optimality system

3.1 The cost-functionals

For our optimality system we consider two cost-functionals; the original as used in the paper [5].

$$J\left(S,I,R,u\right)=\int_{0}^{T}\left[A_{1}S\left(t\right)+A_{2}I\left(t\right)+\frac{\tau}{2}u^{2}\left(t\right)\right]dt \tag{8}$$

and an alternative, strictly convex cost-functional

$$J\left(S,I,R,u\right)=\int_{0}^{T}\left[\frac{A_{1}}{2}S^{2}\left(t\right)+\frac{A_{2}}{2}I^{2}\left(t\right)+\frac{\tau}{2}u^{2}\left(t\right)\right]dt. \tag{9}$$

We also define the reduced cost-functionals as $f\left(u\right))=J\left(SIR(u),u\right)$, where $SIR(u)$ denotes the solution operator for $S(t),I(t)$ and $R(t)$ given a control $u(t)$.

3.2 The control problems

Given the cost-functionals in the section above, the control problems becomes

$$\min_{u\in U_{ad}}f(u) \tag{10}$$

such that the state equation (1) holds and $u\in U_{ad}$, (2).

3.3 Existence of an optimal control $\bar{u}(t)$

To prove the existence of an optimal control, we follow the work in [5]. First we note that the state variables in the state equation (1) are non-negative values, and that the control space (2) is convex and closed by definition. Furthermore the optimal systems are bounded, which determines the compactness needed for the existence of the optimal control. We now only need the necessary convexity of the cost-functionals in $u(t)$ to be satisfied. In both cases (8) and (9), we see that the integrand is convex on the control $u(t)$. Note that the

second case is also convex in $S(t)$ and $I(t)$, making it strictly convex. Continuing on, it is now easy to see that there exist a constant $\rho > 1$, positive numbers ω_1, and ω_2 such that in both cases we have

$$f(u) \geq \omega_2 + \omega_1 \left(|u|^2 \right)^{\rho/2},$$

giving us the existence of an optimal control.

3.4 Deriving the optimality system

To derive the optimality system we define the Lagrangian, L, in both cases as

$$\begin{aligned} &L\left(S, I, R, p_1, p_2, p_3, u\right) = J\left(S, I, R, u\right) \\ &- \int_0^T S_t p_1 dt + \int_0^T \left[-\left(\nu + u\right) S - \tfrac{\beta}{N} SI + N\nu \right] p_1 dt \\ &- \int_0^T I_t p_2 dt + \int_0^T \left[-\left(\gamma + \nu\right) I + \tfrac{\beta}{N} SI \right] p_2 dt \\ &- \int_0^T R_t p_3 dt + \int_0^T \left[\gamma I - \nu R + uS\right] p_3 dt, \end{aligned} \tag{11}$$

where p_1, p_2, p_3 denote the adjoint variables, J is the the cost-functional given in equation (8) or (9), and the rest is given by integrating the state equation (1). We proceed with finding the adjoint equation for our system and deriving the gradients for both cost-functionals under consideration.

3.4.1 Finding the adjoint equation for S

To derive the adjoint equation for S we differentiate the Lagrangian with respect to S, and let $L_S h = 0$, assuming that $h(0) = 0$.

$$\begin{aligned} L_S h &= -\int_0^T p_1 h_t dt + \int_0^T \left[-\left(\nu + u\right) p_1 + u p_3 + \tfrac{\beta}{N} I \left(-p_1 + p_2\right) + A_1 \right] h dt \\ &= \int_0^T \left[-\left(\nu + u\right) p_1 + u p_3 + \tfrac{\beta}{N} I \left(-p_1 + p_2\right) + A_1 \right] h dt \\ &+ p_1(0)h(0) - p_1(T)h(T) + \int_0^T p_{1t} h dt = 0 \end{aligned}$$

Using the assumption that $h(0) = 0$ and the variational lemma (i.e. by first assuming that $h(T) = 0$ and then assuming the contrary), we get

$$\begin{aligned} -p_{1t} &= -\left(\nu + u\right) p_1 + u p_3 + \tfrac{\beta}{N} I \left(-p_1 + p_2\right) + A_1 \\ p_1(T) &= 0. \end{aligned} \tag{12}$$

Note that if we used the alternative cost-functional we would have gotten the term $+A_1 S$ instead of $+A_1$ at the end.

3.4.2 Finding the adjoint equation for I

Following what we did for S, we do the same for I.

$$\begin{aligned}
L_I h &= -\int_0^T p_2 h_t dt + \int_0^T \Big[-(\gamma+\nu) p_2 + \gamma p_3 + \tfrac{\beta}{N} S\left(-p_1 + p_2\right) + A_2 \Big] h dt \\
&= \int_0^T \Big[-(\gamma+\nu) p_2 + \gamma p_3 + \tfrac{\beta}{N} S\left(-p_1 + p_2\right) + A_2 \Big] h dt \\
&+ p_2(0)h(0) - p_2(T)h(T) + \int_0^T p_{2t} h dt = 0
\end{aligned}$$

Now using the assumption that $h(0) = 0$ and the variational Lemma, we get

$$\begin{aligned}
-p_{2t} &= -(\gamma+\nu) p_2 + \gamma p_3 + \tfrac{\beta}{N} S\left(-p_1 + p_2\right) + A_2 \\
p_2(T) &= 0.
\end{aligned} \tag{13}$$

Note that if we used the alternative cost-functional we would got the term $+A_2 I$ instead of $+A_2$ at the end.

3.4.3 Finding the adjoint equation for R

Following what we did for S and I we do the same one last time for R.

$$\begin{aligned}
L_I h &= -\int_0^T p_3 h_t dt + \int_0^T \left[-\nu p_3 \right] h dt \\
&= -\int_0^T \nu p_3 h dt + p_3(0)h(0) - p_3(T)h(T) + \int_0^T p_{2t} h dt = 0
\end{aligned}$$

Now using the assumption that $h(0) = 0$ and the variational Lemma, we find

$$\begin{aligned}
-p_{2t} &= -\nu p_3 \\
p_2(T) &= 0.
\end{aligned} \tag{14}$$

Which we note has the explicit solution $p_3(t) = 0$ for all $t \leq T$.

3.4.4 Finding the Variational inequality and the gradient of the cost-functionals

To find the variational inequality we first derivative the Lagrangian with respect to u, and let $L_u h \geq 0$, where h is a suitable direction.

$$\begin{aligned}
L_u h &= \int_0^T \left[\tau u - S p_1 + S p_3 \right] h dt \\
&\Rightarrow \int_0^T \left[\tau \bar{u} + \bar{S}\left(-\bar{p}_1 + \bar{p}_3\right) \right] (u - \bar{u}) dt \geq 0 \\
&\Rightarrow \left\langle \tau \bar{u} + \bar{S}\left(-\bar{p}_1 + \bar{p}_3\right), u - \bar{u} \right\rangle_{L^2} \geq 0 \\
&\Rightarrow f'(u) = \tau u + S\left(-p_1 + p_3\right)
\end{aligned} \tag{15}$$

Note that using the fact that $p_3(t) = 0$, the gradient of the reduced cost-functional becomes $f'(u) = \tau u - Sp_1$. Note also that the gradient is the same for both of the cost-functionals under consideration.

3.5 The projection operator

Looking at the Variational inequality (15), it is easy to see that the unconstrained problem will be optimal when $f'(\bar{u}) = 0$, meaning that

$$\bar{u}(t) = \frac{\bar{S}(t)(-\bar{p}_1(t) + \bar{p}_3(t))}{\tau}.$$

However, we have a constrained problem. Using the box-constraints defined by the admissible set U_{ad}, (2), we get

$$\bar{u}(t) = \min\left\{0.9, \max\left\{\frac{\bar{S}(t)(-\bar{p}_1(t) + \bar{p}_3(t))}{\tau}, 0\right\}\right\}.$$

This defines our projection operator as

$$Proj_{U_{ad}}(x) = \min\left\{0.9, \max\left\{x, 0\right\}\right\}. \tag{16}$$

3.6 The optimality system

Using the results from the previous sections, we define

$$A(u) = \begin{bmatrix} -(\nu + u) & 0 & 0 \\ 0 & -(\gamma + \nu) & 0 \\ u & \gamma & -\nu \end{bmatrix}, \mathbf{F}(\mathbf{y}) = \begin{bmatrix} -\frac{\beta}{N} SI + N\nu \\ \frac{\beta}{N} SI \\ 0 \end{bmatrix},$$
$$J_F(\mathbf{y}) = \frac{\beta}{N} \begin{bmatrix} -I & -S & 0 \\ I & S & 0 \\ 0 & 0 & 0 \end{bmatrix}, \mathbf{b}_1 = \begin{bmatrix} A_1 \\ A_2 \\ 0 \end{bmatrix}, \mathbf{b}_2(\mathbf{y}) = \begin{bmatrix} A_1 S \\ A_2 I \\ 0 \end{bmatrix},$$

where $\mathbf{y}(t) = \begin{bmatrix} S(t) & I(t) & R(t) \end{bmatrix}^\top$ and $J_F(\mathbf{y})$ is the Jacobian matrix of $\mathbf{F}(\mathbf{y})$.

This gives us the state equations (1), adjoint equations and the gradient as

$$\begin{aligned} \mathbf{y}'(t) &= A(u)\mathbf{y}(t) + \mathbf{F}(\mathbf{y}(t)) \quad , \quad \mathbf{y}(0) = \mathbf{y}_0, \\ -\mathbf{p}'(t) &= A(u)\mathbf{p}(t) + J_F(\mathbf{y})\mathbf{p}(t) + \mathbf{b} \quad , \quad \mathbf{p}(T) = 0, \\ f'(u) &= \tau u + S(-p_1 + p_3), \end{aligned} \tag{17}$$

where $\mathbf{y}_0 = \begin{bmatrix} S_0 & I_0 & R_0 \end{bmatrix}^\top$, $\mathbf{p}(t) = \begin{bmatrix} p_1(t) & p_2(t) & p_3(t) \end{bmatrix}^\top$ and $\mathbf{b} = \mathbf{b_1}$ given the original cost functional (8) and $\mathbf{b} = \mathbf{b}_2(\mathbf{y})$ given the alternative cost functional (9).

4 Numerical experiment

4.1 Method

4.1.1 The projected gradient method

To solve the optimality system given in (17), we use a projected gradient method, meaning that the search direction is projected onto the admissible set U_{ad}, (2). Here we use the aforementioned forward-time RK4 method to solve the state equation, and a backward-time RK4 method to solve the adjoint equation. We also use Armijo backtracking to find the step-size with which to move along our search-direction. The method stops either when the step-size is to small, the maximum number of iterations is reached or when $||u_{k+1} - u_k||_{L^2} < tol$, where tol is some user-specified tolerance.

4.1.2 Input parameters

For solving the optimal control problem using both cost-functionals, we chose an endtime of $T = 100$ and $M = 10000$ timesteps. Inspired by an example in the article by Gul Zaman, Yong Han Kang and Il Hyo Jung, [5], we choose the initial conditions $S_0 = 700$, $I_0 = 165$ and $R_0 = 90$, yielding a total population of $N = 955$. We also set the birth and death rate to $\nu = 0.41$, the recovery rate $\gamma = 0.56$ and the transmission coefficient to $\beta = 0.002$. Next, we need to decide the parameters A_1, A_2 and τ for the two cost-functionals, which gives the cost associated with people being susceptible, infected and the cost of vaccination, respectively. For the original cost-functional, the parameter values $A_1 = 0.050, A_2 = 0.075$ and $\tau = 15$ will be used. For the alternative cost-functional it is natural to scale A_1, A_2 by N, so we set $A_1 = 0.050/N \cdot 2.95, A_2 = 0.075/N \cdot 2.95$ and $\tau = 14$, where the factor of 2.95 is needed to obtain convergence. Moreover, for both control problem we use the tolerance $tol = 10^{-6}$.

4.2 Results & Discussion

4.2.1 Using the original cost-functional

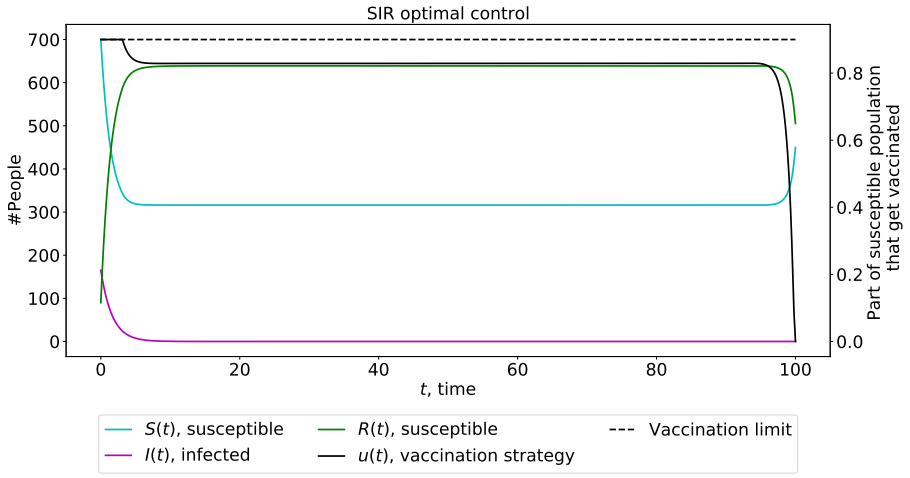

Figure 3: State variables and vaccination strategy, using the original cost-functional

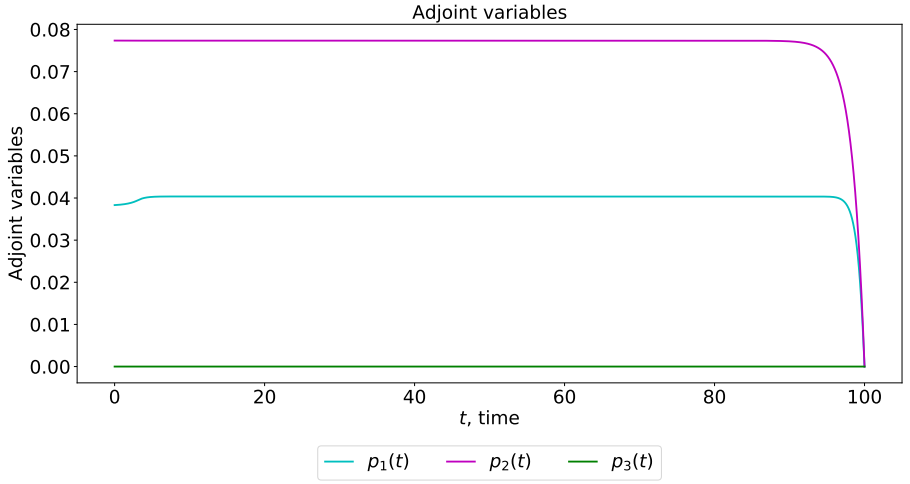

Figure 4: Adjoint variables, using the original cost-functional

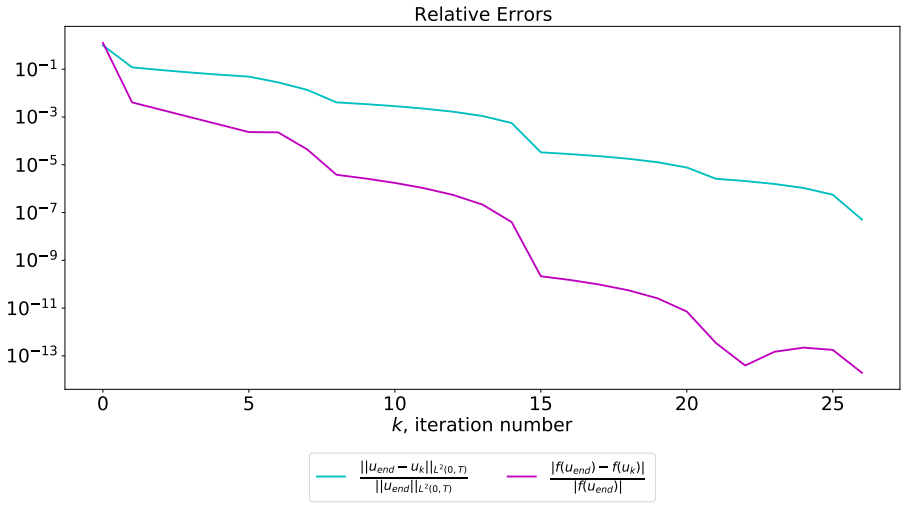

Figure 5: Relative errors, using the original cost-functional. $k = 0, \cdots, k_{end} - 1$

Looking at the Figures above, we see that the optimal vaccination strategy consists of vaccinating at maximal capacity $u(t) = 0.9$ at the start, but then quickly reducing the vaccinations slightly. As a consequence of this we have full vaccination in the start and a large portion of those susceptible get vaccinated before they have a chance to get infected. As such, the number of susceptible and infected people drops down quickly. Once the number of infected people is close to zero, the optimal vaccination strategy has dropped down from 0.9 to 0.8, remaining constant for some time. In the end there are very few infected people- presumably due to the emergence of herd immunity- so vaccination is no longer needed. Due to this drastic decrease in vaccinations, the number of susceptible people starts increasing and the number of recovered people starts diminishing as new people are born into the population without being vaccinated, and old immune people starts dying and leaving the population, all due to our nonzero birth/death rate. This behaviour is in line with what we expected after having read the article by Gul Zaman, Yong Han Kang and Il Hyo Jung, [5].

Note, however, that there are some differences in our results versus those of the article. We observe some difference in the time-evolution of the state variables, however more pronounced is the difference in the adjoint variables, and in particular, the difference in $p_1(t)$. Specifically, it does not appear to be a quadratic polynomial, as we would expect from the article by Gul Zaman, Yong Han Kang and Il Hyo Jung, [5].

Looking at the figure for the relative error we see that both the L^2-norm of the vaccination strategy u_k and the value of the reduced cost-functional $f(u_k)$ decreases as we iterate through the values of k. We also observe that the slopes of both these curves are comparable, except for the last few iterations. Here we observe that the relative norm of the cost-functional in fact increases slightly

before finally reaching the minimum for our prescribed tolerance level.

4.2.2 Using the alternative cost-functional

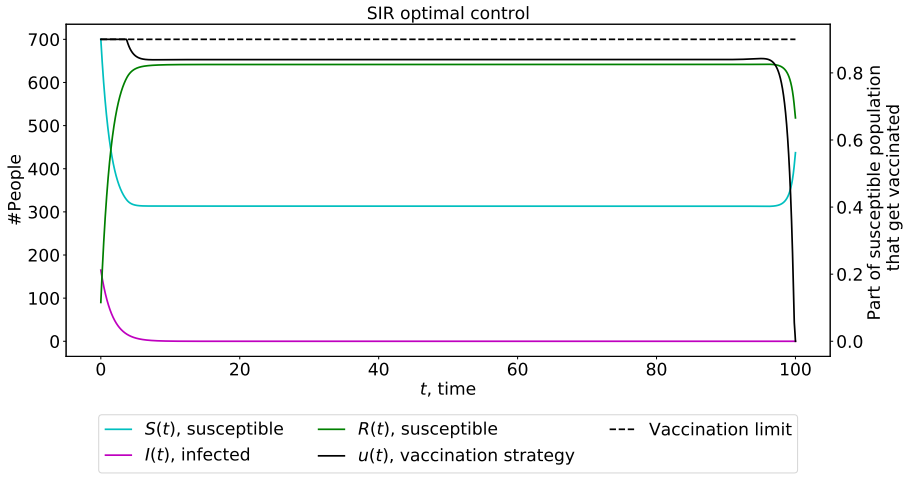

Figure 6: State variables and vaccination strategy, using the alternative cost-functional

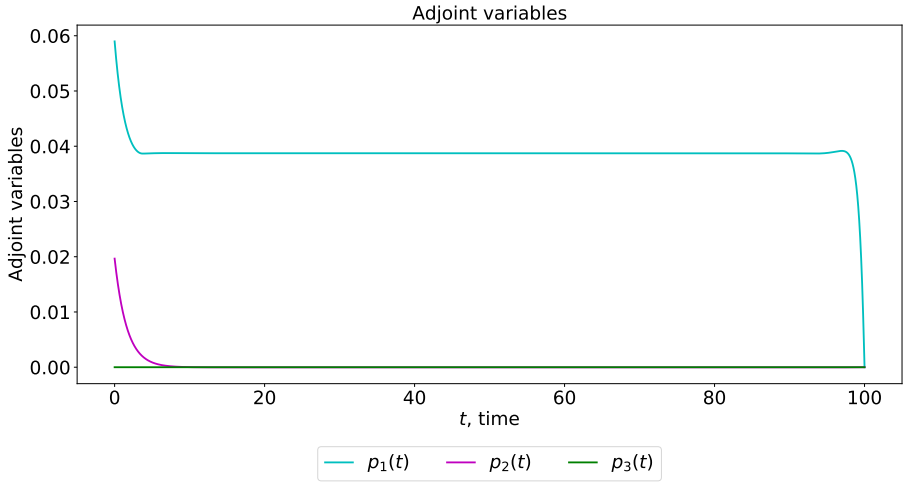

Figure 7: Adjoint variables, using the alternative cost-functional

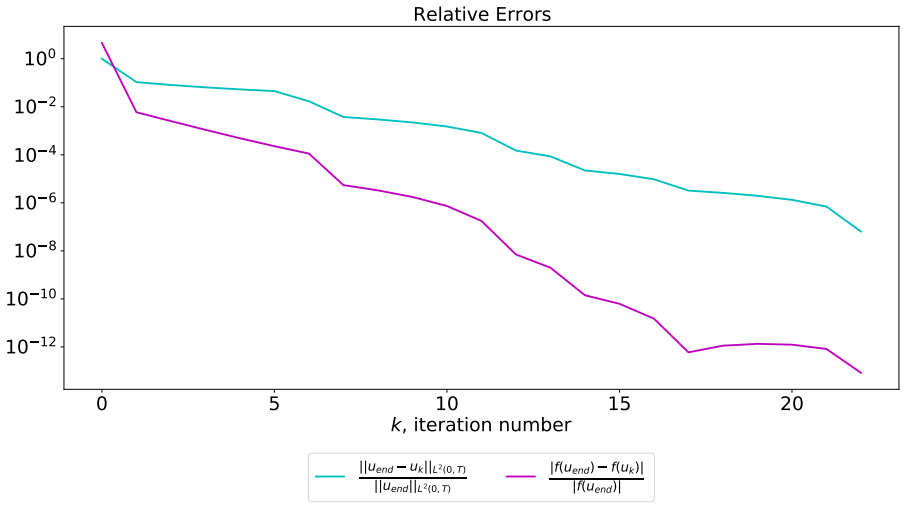

Figure 8: Relative errors, using the alternative cost-functional.
$k = 0, \cdots, k_{end} - 1$

Turning our attention to the alternative cost-functional, we observe more or less the same results both for the evolution of the state variables, and for the optimal vaccination strategy as we did with the original cost-functional. However, there is a large difference in the adjoint variables $p_1(t)$ and $p_2(t)$ for the two cost-functionals. We observe in particular that $p_2(t)$ rapidly joins $p_3(t)$ at zero, whereas p_1 starts out quite large before stabilizing around the same constant value as for the original cost-functional. In a sense, $p_1(t)$ looks more like a cubic polynomial. A difference here is expected since we have two quite different cost-functionals we are working with. In particular, the factor difference of $+A_1$ against $+A_1 S$, and $+A_2$ against $+A_2 I$ should have some effect.

4.2.3 Convergence and choice of parameter values

Unfortunately, we experienced that the projected gradient method failed to converge for a plethora of choices for parameters A_1, A_2 and τ. We found experimentally that $\tau > 50$ is typically required for convergence, which corresponds to a quite large cost associated with vaccination. Furthermore, for both cost-functionals (and in particular, the non-scaled alternative cost-functional) we require $A_1 \leq 0.060$ and $A_1 \leq A_2$. The latter point seems very reasonable, as we would expect the cost of keeping infected people in your population to be much higher than the cost of keeping susceptible people in your population. Among potential values for τ which could yield convergence, we have chosen a rather small value because otherwise the optimal vaccination strategy does not include vaccinating at full capacity right at the start of the outbreak, a feature we found interesting and wished to display.

In light of the preceding discussion, we also wanted to explore the effect of different optimization routines. In particular, we wanted to implement a Quasi-Newton method (e.g. BFGS) to see if this would permit convergence with parameter values currently not supported by the projected gradient descent method. Unfortunately, we did not have time to implement and test this. Further extensions to this project could be implementing time-dependent constraints on the form

$$U_{ad} = \{u(t) : \text{u is measurable and } u_a(t) \leq u(t) \leq u_b(t) \text{ for all t}\},$$

where $u_a(t)$ and $u_b(t)$ are functions. This was implemented, but we didn't have time to test it due to the convergence problems previously outlined.

5 Conclusion

The projected gradient method is successful at generating an optimal vaccine strategy similar to those discovered in earlier work. Unfortunately, the optimal vaccine strategy outlined and tested herein does not appear suitable for the case of an outbreak of a novel disease, the optimal vaccination strategy presupposes that the vaccine is available immediately once the outbreak starts. This may not be the case for different constraints on the control, however we did not have time to investigate this further. Thus, the strategy developed here can at best be said to be suitable for predictable outbreaks, e.g. the seasonal flu. Furthermore, the choice of cost-functional seems to have little effect on the final result. The biggest flaw of the experiment is the inability of the system to converge for any choice of parameters in the cost-functional. Investigating other optimization methods (e.g. Quasi-Newton methods) might improve upon our convergence issues.

References

[1] Michael te Vrugt, Jens Bickmann, Raphael Wittkowski. *Effects of social distancing and isolation on epidemic spreading modeled via dynamical density functional theory* 2020, Nature Communications 11

[2] Alfio Quarteroni, Riccardo Sacco and Fausto Saleri *Numerical Mathematics, Second Edition*, 2007, avalible from `https://www.springer.com/gp/book/9783540346586`

[3] Statistics Norway (11.03.2021). Deaths. *ssb.no*. Retrieved from `https://www.ssb.no/en/befolkning/fodte-og-dode/statistikk/dode`

[4] Statistics Norway (11.03.2021). Births. *ssb.no*. Retrieved from `https://www.ssb.no/en/fodte`

[5] Gul Zaman, Yong Han Kang and Il Hyo Jung, *Stability analysis and optimal vaccination of an SIR epidemic model*, 2008, available from `https://www.sciencedirect.com/science/article/abs/pii/S0303264708001044`